

Author's Accepted Manuscript

Trabecular orientation in the Human femur and tibia and the relationship with lower-limb alignment for patients with osteoarthritis of the knee

Shameem A. Sampath, Sandra Lewis, Matteo Fosco, Domenico Tigani



PII: S0021-9290(15)00044-5
DOI: <http://dx.doi.org/10.1016/j.jbiomech.2015.01.028>
Reference: BM6993

To appear in: *Journal of Biomechanics*

Accepted date: 25 January 2015

Cite this article as: Shameem A. Sampath, Sandra Lewis, Matteo Fosco, Domenico Tigani, Trabecular orientation in the Human femur and tibia and the relationship with lower-limb alignment for patients with osteoarthritis of the knee, *Journal of Biomechanics*, <http://dx.doi.org/10.1016/j.jbiomech.2015.01.028>

This is a PDF file of an unedited manuscript that has been accepted for publication. As a service to our customers we are providing this early version of the manuscript. The manuscript will undergo copyediting, typesetting, and review of the resulting galley proof before it is published in its final citable form. Please note that during the production process errors may be discovered which could affect the content, and all legal disclaimers that apply to the journal pertain.

SHORT COMMUNICATION**Trabecular orientation in the human femur and tibia and the relationship with lower-limb alignment for patients with osteoarthritis of the knee**

Shameem A Sampath ^a, Sandra Lewis ^b, Matteo Fosco ^c, Domenico Tigani ^d

^a The Bluespot Knee Clinic, 32 Orchard Road, Lytham, Lancashire, United Kingdom

^b Manchester Metropolitan University, Crewe Green Road, Crewe, United Kingdom

^c Rizzoli Orthopaedic Institute, University of Bologna, Via Pupilli 1, 40136 Bologna, Italy

^d Orthopaedic Surgery, Santa Maria alle Scotte Hospital, viale Bracci 1, 53100, Siena, Italy

Corresponding author: Dr Sandra Lewis

Address: Manchester Metropolitan University, Crewe Green Road, Crewe, CW1 5DU, UK; Tel: +44

161 247 5765; Fax: +44 161 247 6375; Email: s.lewis@mmu.ac.uk

Word count for manuscript: 2,481

Key words: knee; trabeculae; alignment; mechanical axis

Abstract

Wolff's Law suggests that the orientation of trabeculae in human bone changes in response to altered loading patterns. The aim of this study was to investigate the trabecular orientation in both the femur and tibia and to compare this with the mechanical axis of the leg. The study involved analysis of radiographs from patients with osteoarthritis of the knee ($n = 91$). For each patient, the trabecular orientation in both the distal femur and proximal tibia were measured from a standard anteroposterior radiograph of the knee and the mechanical axis of the leg was calculated from a long leg view taken while weight bearing. There was a significant correlation between the mechanical axis and the trabecular orientation in each of the regions considered in the femur ($r = -0.41, -0.30, 0.52, 0.23$) and tibia ($r = -0.27, 0.31$). Multiple regression analysis, with mechanical axis as the dependent variable, produced an R^2 of 0.62. Greater trabecular anisotropy (i.e. greater alignment) was observed in the medial femur and tibia compared to the lateral side ($p < 0.01$). The results give an insight into the trabecular changes that may take place during development of osteoarthritis and following surgery. In particular, we propose that the orientation of the trabeculae in both the distal femur and proximal tibia will reflect the angle of mechanical loading through the knee.

Introduction

Bone tissue is influenced by its mechanical environment and adapts in response to applied forces. This concept is known as Wolff's Law, as a result of the seminal work carried out in this field by Julius Wolff in the late 19th century (Wolff, 1892). *A key element of Wolff's proposal was the hypothesis that trabeculae within bone align with the principal lines of stress.*

The aim of our study was to investigate the trabecular orientation in the distal femur and proximal tibia in patients with osteoarthritis (OA) and compare this with the mechanical axis of the lower limb. The direction of force through the lower limb varies in line with the mechanical axis and hence we hypothesized that there would be a correlation between the trabecular orientation and the mechanical axis.

Patients and Methods

Ethical approval for the study was granted by Manchester Metropolitan University Ethics Committee. The radiographs were obtained from an Orthopaedic Clinic in Italy and involved patients with OA of the knee prior to Total Knee Arthroplasty (TKA). All radiographs were taken in the course of normal clinical practice and patients gave consent for the images to be analysed for research purposes.

The study involved anonymised radiographs from 90 patients. Each patient had both a standard anteroposterior radiograph of the knee and a long leg view taken while weight bearing, and fifteen patients had radiographs for both knees. Nine radiographs were excluded as either the femoral head or tibial plafond (in the case of the long leg view) or the tibial or femoral outer margins (in the case of the anteroposterior radiographs) were not completely visible or the images were considered too blurry. Three further radiographs were excluded from the orientation analysis because the extreme angle of the tibia prevented a horizontal rectangle of sufficient size being drawn between the sclerotic bone and the growth line. The analysis was therefore based on 93 radiographs (28 from males and 65 from females). The mean age (\pm standard deviation (SD)) was 67.5 (\pm 8.0) years (range 49 – 80 years).

The radiographs were obtained using a Philips OmniDiagnost Eleva multifunctional remote control Digital Radiography (DR) system with the patient erect in anteroposterior 110 cm from the radiographic tube. Pixel resolution was 0.61 x 0.61mm for long leg images and 0.17 x 0.17mm for anteroposterior. A full-length leg filter was placed on the lower half of the tube to prevent overexposure at the ankles. Settings of 85-100 kV and 160–320 mA/s were employed, depending on the patient's bodyweight.

All radiographs were analysed using ImageJ (Rasband, 1997-2012), which is Java based software for medical image analysis. The alignment of the trabeculae in all areas of interest was assessed using OrientationJ (Rezakhaniha et al., 2012), which is a plug-in for use with ImageJ. OrientationJ uses structure tensors to determine the dominant trabecular orientation in an outlined area. For this purpose, it has an advantage over fractal signature analysis which only measures trabecular structure in the horizontal and vertical directions (although Wolski et al. (2009) have recently developed directional fractal signature methods to address this issue). More details regarding OrientationJ are given in Rezakhaniha et al., 2012. Prior to our analysis, the validity of OrientationJ measurements was confirmed by testing a number of sample images of known orientation. OrientationJ also returns a coherency figure, which is a measure of the anisotropic properties of the region of interest. The coherence is 1 when the local structure has one dominant orientation and 0 if the image is essentially isotropic.

Statistical analysis was conducted using SPSS software (version 20.0). Intra- and inter- tester reliability analyses (using intraclass correlations (ICC) [type 2,1]) were carried out on the angle, orientation and coherency measurements. Three testers with backgrounds in biomechanics were trained on the method. Each then measured the full batch of images twice, with a minimum of a week's interval between testing sessions. A one-way independent analysis of variance (ANOVA) was performed on the orientation results, split by mechanical axis, and pairwise comparisons were performed using a Bonferroni correction. One-tailed correlational analysis was performed between the mechanical axis and the angle of the trabeculae for each of the regions considered. These results were used as a basis for a stepwise regression analysis with the mechanical axis as the dependent variable. The anisotropy of the medial and lateral regions was compared using dependent t-tests.

Mechanical axis

The mechanical axis of the lower limb was measured from the full length radiographs using the method devised and validated on ImageJ software by Goker and Block (2007). This approach involves calculating the angle formed by the femoral and tibial axes. A line is drawn from the centre of the femoral head to the intercondylar notch and a second line is drawn from the tibial interspinous groove to the centre of the tibial plafond (Figure 1).

Figure 1

The mechanical axis is then calculated as the angle between these two lines, where varus is taken as positive and valgus negative (Figure 2).

Figure 2

FS and TS angles

For each anteroposterior radiograph, the angle of the femoral shaft (FS) and tibial shaft (TS) were calculated from the femoral intercondylar point to the mid-point of the femoral shaft and from the

tibial interspinous point to the mid-point of the tibial shaft respectively. In each case, the point of the shaft was taken to be the furthest point that was visible on the radiograph. While this inevitably led to a slight variation between patients, it maintained the simplicity and clinical relevance of the measurements and was not considered to materially affect the results.

Orientation measurements

Within the medial tibia, a rectangle was selected with the borders being the subchondral cortex, the growth line, the outer margin and the centre of the medial tibial spine. By running a specifically designed macro, the middle half of this rectangle was split into an upper and lower region. In this way, the outer quarter was excluded which avoided the periarticular osteopenia adjacent to osteophyte formation (Podsiadlo et al., 2008). Orientation measurements were taken in both regions. The same rectangle was then moved to the lateral side of the tibia and both the medial and lateral femur and lined up with the subchondral cortex and outer margins. In each case, the macro was run to create an upper and lower region and orientation measurements were taken in both. The analysis was therefore based on four outer rectangles (medial femur, lateral femur, medial tibia and lateral tibia), each one containing an upper and a lower region of interest (Figure 3).

Figure 3

In all cases the medial and lateral orientation angles were expressed relative to the angle of the femoral or tibial shaft as appropriate (Figure 4). This method of calculation meant that some angles were negative and possible angles ranged from -180° to 180° .

Figure 4

In order to illustrate the expected results following from our hypothesis, Figure 5 represents a simplified diagram of two left knees; one neutral and one varus. In a neutral knee the joint reaction forces would be expected to be broadly in line with the angle of the femur and tibia. However, in both varus and valgus knees, the reaction forces would be at an angle to the axis of the bone. The angle shown represents the anticipated angle of the joint reaction force in the lateral femur relative to the bone axis. If trabecular orientation is in line with the joint reaction force, as hypothesized, then this trabecular angle would be expected to be greater with a varus knee than a neutral one. In the medial compartment the trabecular orientation (relative to the bone axis) would be expected to be smaller or negative. Since the mechanical axis is positive for a varus knee, a positive correlation would be anticipated for the lateral side and a negative one for the medial. In the tibia of a varus knee, this would be reversed. The direction of the correlations are hypothesized to be the same for valgus knees since the mechanical axis is negative in this case.

Figure 5

Results

Reliability

In most cases, both intra-tester and inter-tester analysis demonstrated good to excellent reliability (ICC > 0.70) (Table 1). However, for both the upper tibial regions, the reliability of the inter-tester orientation measurements was noticeably lower (ICCs of 0.53 and 0.55). These measurements also showed a higher SD across all radiographs than for the other regions, possibly due to the presence of sclerotic areas. As a result, the measurements for the upper tibia were considered unreliable and hence were not used in the correlational or regression analysis. The following analysis was therefore based on the six remaining regions.

Mechanical axis and trabecular orientation

One patient (who had images of both knees) was considered to be an outlier. The measurements from these two radiographs were therefore excluded and so the results are based on analysis of 91 knees. Figure 6 illustrates the mean trabecular orientation measurements when the radiographs were split by mechanical axis. There was a significant difference in the trabecular orientation between these groups for the upper lateral femoral region, both medial femoral regions and the lower medial tibial region. The significant pairwise comparisons (after applying a Bonferroni correction) are shown in Figure 6.

Figure 6

A two-tailed test showed that the lower medial orientation measure in the tibia was significantly higher for females than for males ($p < 0.01$). None of the other measures varied significantly between the sexes. As shown in Table 2, there was a significant correlation between the mechanical axis and the trabecular orientation in all of the six regions considered. Age was not correlated with either mechanical axis or trabecular orientation.

Table 2

The results of the overall correlational analysis were used to guide selection in a stepwise multiple regression analysis with mechanical axis as the dependant variable. The optimal model included five of the measurements as independent variables and the total R^2 was 0.62 as shown in Table 3.

Table 3

Anisotropy

The coherence of the each medial area was compared to the coherence of each corresponding lateral area. In all cases (excluding the upper tibia), the coherence on the medial side was significantly greater (indicating greater anisotropy) than on the lateral side ($p < 0.01$ in each case).

Discussion

This study found significant correlations between the mechanical axis and trabecular orientation in both the distal femur and proximal tibia. In all regions considered, the direction of the correlations was in line with the original hypothesis and reflected the expected angle of loading relative to the axis of the bone (Figure 5). The results were therefore consistent with Wolff's Law, which proposes that trabecular bone adapts in response to mechanical loading.

The dynamic realignment of trabecular bone in response to changes in joint loading has been supported by recent animal studies in which guinea fowl and sheep were exercised on inclined treadmills and a close correspondence was found between the change in joint angle and the subsequent difference in trabecular orientation (Pontzer et al., 2006; Barak et al., 2011). Alternative approaches, using biomechanical models, have also *supported* the hypothesis that trabecular orientation reflects and adapts to external loads. This has been shown, both when analysing bone microstructure in response to different loading conditions (e.g. Wang et al., 2012) and also, on a larger scale, when modelling stress patterns and trabecular structure in the human femur (Boyle & Kim, 2011; Tsubota et al., 2009) and calcaneus (Gefen & Seliktar, 2004).

It has been suggested that tibial trabeculae in osteoarthritic knees are aligned more vertically than in healthy knees (Kamibayashi et al., 1995; Podsiadlo et al., 2008), possibly due to a loss of shock-absorbing cartilage and greater bone-on-bone compressive forces (Kamibayashi et al., 1995). This proposal followed from the results of study by Kamibayashi et al. (1995), who compared trabecular orientation in tibial bone samples from patients with OA and age-matched controls. However, sample sizes were limited and measurements were only taken from the medial (and not the lateral) condyle. More research to investigate precise trabecular orientation in the human tibia would therefore be beneficial.

Anisotropy is generally thought to be lower when OA is present (Ding et al., 2003; Podsiadlo et al., 2008; Wolski et al., 2010), suggesting that weaker anisotropy may be a consequence of the changes in loading environment in osteoarthritic knees (Podsiadlo et al., 2008). In the current study, greater trabecular anisotropy was observed in the medial femur and tibia compared to the lateral side. As most of the patients had varus alignment, they would be expected to have greater medial compressive loads, whereas, on the lateral side, shear stresses may play a relatively greater role. Since trabecular orientation is hypothesized to align with the direction of the applied loads, a less dominant compressive load may lead to greater 'disorganisation' of the trabecular structure. This is consistent with the results of a 3D simulation which showed greater anisotropy when loads were applied primarily in a vertical direction rather than equally horizontally and vertically (Wang et al., 2012).

To the best of the authors' knowledge, this is the first study to investigate the relationship between leg alignment and trabecular orientation in human knees. The results give an insight into the trabecular changes that may occur following medical conditions, injury, surgery or ageing; all of which may influence the mechanical axis and hence the direction and magnitude of stress on the bone. In OA of the knee, this is particularly important in order to better understand the changes that occur during development of the condition and subsequent bone remodelling following surgery and prosthetic implant. In addition, simple measurements of trabecular orientation that can be taken from clinical anteroposterior radiographs might provide valuable pre-operative information on the mechanical loading environment if full leg, weight-bearing images are not available.

Limitations

This study is based on 2D measurements and relates these to 3D microarchitecture within the bone. There is therefore inevitably a source of error within this method, although it has been shown that measures of trabecular architecture taken from 2D radiographs can have a high correlation with 3D measures (e.g. Luo et al., 1999; Steines et al., 2009). Body weight has previously been shown to affect trabecular bone structure (e.g. Andersen et al., 2014). Unfortunately BMI data was not available for the patients in this study, but the results showed that significant relationships exist between mechanical axis and trabecular orientation within a typical patient group of mixed body weight. The study also did not include an analysis of the effects of different radiographic measuring conditions. Nevertheless, the method was found to produce reliable results within a standard batch of clinical anteroposterior knee radiographs (incorporating images of varying quality). This study represents our preliminary findings prior to more detailed investigation involving 3D analysis. However, the simplicity of this technique means that it offers a quick, freely available measure that can be applied to standard clinical radiographs.

Acknowledgements

The authors would like to thank Dr Casey Lee and Clare Dadswell at Manchester Metropolitan University for their participation as testers in the reliability analysis.

Conflict of interest statement

No conflict of interest reported by any author.

References

- Andersen, S., Frederiksen, K.D., Hansen, S., Brixen, K., Gram, J., Støving, R.K., 2014. Bone structure and estimated bone strength in obese patients evaluated by high-resolution peripheral quantitative computed tomography. *Calcif. Tissue Int.* 95, 19-28.
- Barak, M.M., Lieberman, D.E., Hublin, J.-J., 2011. A Wolff in sheep's clothing: trabecular bone adaption in response to changes in joint loading orientation. *Bone* 49, 1141-1151.
- Boyle C., Kim I.Y., 2011. Three-dimensional micro-level computational study of Wolff's law via trabecular bone remodelling in the human proximal femur using design space topology optimization. *J. Biomech.* 44, 935-942.
- Ding, M., Odgaard, A., Hvid, I., 2003. Changes in the three-dimensional microstructure of human tibial cancellous bone in early osteoarthritis. *J. Bone Joint Surg. Br.* 85, 906-912.
- Gefen, A., Seliktar, R. 2004. Comparison of the trabecular architecture and the isostatic stress flow in the human calcaneus. *Med. Eng. Phys.* 26, 119-129.
- Goker, B., Block, J., 2007. Improved precision in quantifying knee alignment angle. *Clin. Orthop. Relat. R.* 458, 145-149.
- Kamibayashi, L., Wyss, U.P., Cooke, T.D.V., Zee, B., 1995. Changes in mean trabecular orientation in the medial condyle of the proximal tibia in osteoarthritis. *Calcified Tissue Int.* 57, 69-73.
- Luo, G., Kinney, J.H., Kaufman, J.J., Haupt, D., Chiabrera, A., Siffert, R.S., 1999. Relationship between plain radiographic patterns and three-dimensional trabecular architecture in the human calcaneus. *Osteoporos. Int.* 9, 339-345.
- Podsiadlo, P., Dahl, L., Englund, M., Lohmander, L.S., Stachowiak, G.W., 2008. Differences in trabecular bone texture between knees with and without radiographic osteoarthritis detected by fractal methods. *Osteoarthr. Cartilage* 16, 323-329.
- Pontzer, H., Lieberman, D.E., Momin E., Devlin, M.J., Polk, J.D., Hallgrímsson, B., Cooper, D.M.L., 2006. Trabecular bone in the bird knee responds with high sensitivity to changes in load orientation. *J. Exp. Biol.* 209, 57-65.
- Rasband, W.S., 1997-2012. ImageJ, U. S. National Institutes of Health, Bethesda, Maryland, USA, <http://imagej.nih.gov/ij>.
- Rezakhaniha, R., Agianniotis, A., Schrauwen, J.T.C., Griffa, A., Sage, D., Bouten, C.V.C., van de Vosse, F.N., Unser, M., Stergiopoulos, N., 2012. Experimental investigation of collagen waviness and orientation in the arterial adventitia using confocal laser scanning microscopy. *Biomech. Model Mechan.* 11, 461-473.
- Steines, D., Liew, S-W., Arnaud, C., Vargas-Voracek, R., Nazarian, A., Müller, R., Snyder, B., Hess, P., Lang, P., 2009. Radiographic trabecular 2D and 3D parameters of proximal femoral bone cores correlate with each other and with yield stress. *Osteoporos. Int.* 20, 1929-1938.
- Tsubota, K., Suzuki, Y., Yamada, T., Hojo, M., Makinouchi, A., Adachi, T., 2009. Computer simulation

of trabecular remodelling in human proximal femur using large-scale voxel FE models: approach to understanding Wolff's law. *J. Biomech.* 42, 1088-1094.

Wang, H., Ji, B., Liu, X.S., Guo, X.E., Huang, Y., Hwang, K-C., 2012. Analysis of microstructural and mechanical alterations of trabecular bone in a simulated three-dimensional remodeling process. *J. Biomech.* 45, 2417-2425.

Wolff, J., 1892. *Das Gesetz der Transformation der Knochen*. Berlin: Hirschwald Verlag.

Wolski, M., Podsiadlo, P., Stachowiak, G.W., 2009. Directional fractal signature analysis of trabecular bone: evaluation of different methods to detect early osteoarthritis in knee radiographs. *Proc. Inst. Mech. Eng. H.* 223, 211-236.

Wolski, M., Podsiadlo, P., Stachowiak, G.W., Lohmander, L.S., Englund, M., 2010. Differences in trabecular bone texture between knees with and without radiographic osteoarthritis detected by directional fractal signature method. *Osteoarthr. Cartilage* 18, 684-690.

Accepted manuscript

Table 1

Intraclass correlation coefficients (ICC) and confidence intervals (CI) for intra-tester and inter-tester reliability analysis

	Intra-tester ICC (95% CI)	Inter-tester ICC (95% CI)
Mechanical axis	0.996 (0.994, 0.997)	0.95 (0.93, 0.97)
Trabecular Orientation - Distal Femur		
Medial upper region	0.84 (0.77, 0.89)	0.74 (0.65, 0.81)
Medial lower region	0.86 (0.79, 0.91)	0.77 (0.69, 0.84)
Lateral upper region	0.83 (0.75, 0.88)	0.72 (0.62, 0.80)
Lateral lower region	0.87 (0.81, 0.91)	0.73 (0.63, 0.81)
Trabecular Orientation - Proximal Tibia		
Medial upper region*	0.64 (0.50, 0.75)	0.53 (0.41, 0.65)
Medial lower region	0.88 (0.82, 0.92)	0.73 (0.64, 0.81)
Lateral upper region*	0.77 (0.67, 0.84)	0.55 (0.43, 0.67)
Lateral lower region	0.79 (0.70, 0.86)	0.70 (0.60, 0.78)
Coherence - Distal Femur		
Medial upper region	0.89 (0.84, 0.93)	0.88 (0.80, 0.92)
Medial lower region	0.87 (0.80, 0.91)	0.84 (0.77, 0.89)
Lateral upper region	0.88 (0.82, 0.92)	0.83 (0.74, 0.89)
Lateral lower region	0.90 (0.84, 0.93)	0.83 (0.75, 0.89)
Coherence - Proximal Tibia		
Medial upper region*	0.84 (0.76, 0.89)	0.64 (0.53, 0.74)
Medial lower region	0.92 (0.87, 0.95)	0.61 (0.49, 0.71)
Lateral upper region*	0.79 (0.69, 0.86)	0.73 (0.63, 0.81)
Lateral lower region	0.86 (0.79, 0.91)	0.71 (0.61, 0.79)

* The measurements from these regions were considered unreliable and therefore excluded from further analysis

Table 2

Correlational coefficients between mechanical axis and trabecular orientation

	Correlation with mechanical axis	p value
Distal Femur		
Medial upper region	-0.41	<0.01
Medial lower region	-0.30	<0.01
Lateral upper region	0.52	<0.01
Lateral lower region	0.23	0.03
Proximal Tibia		
Medial lower region	0.31	<0.01
Lateral lower region	-0.27	0.01

Accepted manuscript

Table 3

Stepwise regression analysis with mechanical axis as the dependent variable

Variable	R²	R² change	Standardised β
Femur - lateral upper	0.27	0.27	0.42
Tibia - lateral lower	0.44	0.17	-0.40
Tibia - medial lower	0.48	0.04	0.42
Femur - medial lower	0.60	0.12	-0.31
Femur - medial upper	0.62	0.02	-0.19

Accepted manuscript

Figure 1: A full length radiograph showing calculation of the mechanical axis of the left leg using Image J software.

Figure 2: Schematic diagram showing method for calculating mechanical axis.

Figure 3: Anteroposterior radiograph of the knee showing the eight regions for which orientation measurements were taken.

Figure 4: Anteroposterior radiograph of the knee showing calculation of the lateral femoral orientation angle. The angle was expressed relative to the angle of the femoral shaft as shown in blue. Possible angles ranged from -180° to 180° .

Figure 5: A simplified diagram of two left knees; one neutral and one varus showing the expected direction of the reaction forces and the angle relative to the angle of the bone.

Figure 6: Mean trabecular orientation (and 95% confidence intervals of the mean) in each region, split into 4 groups by mechanical axis. Pairwise significant differences between groups (after Bonferroni correction) are shown by a *.

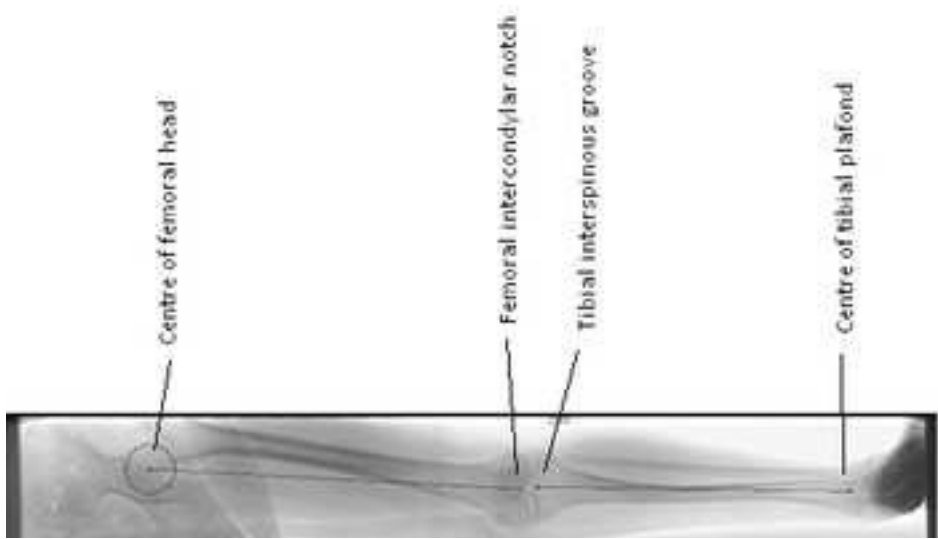
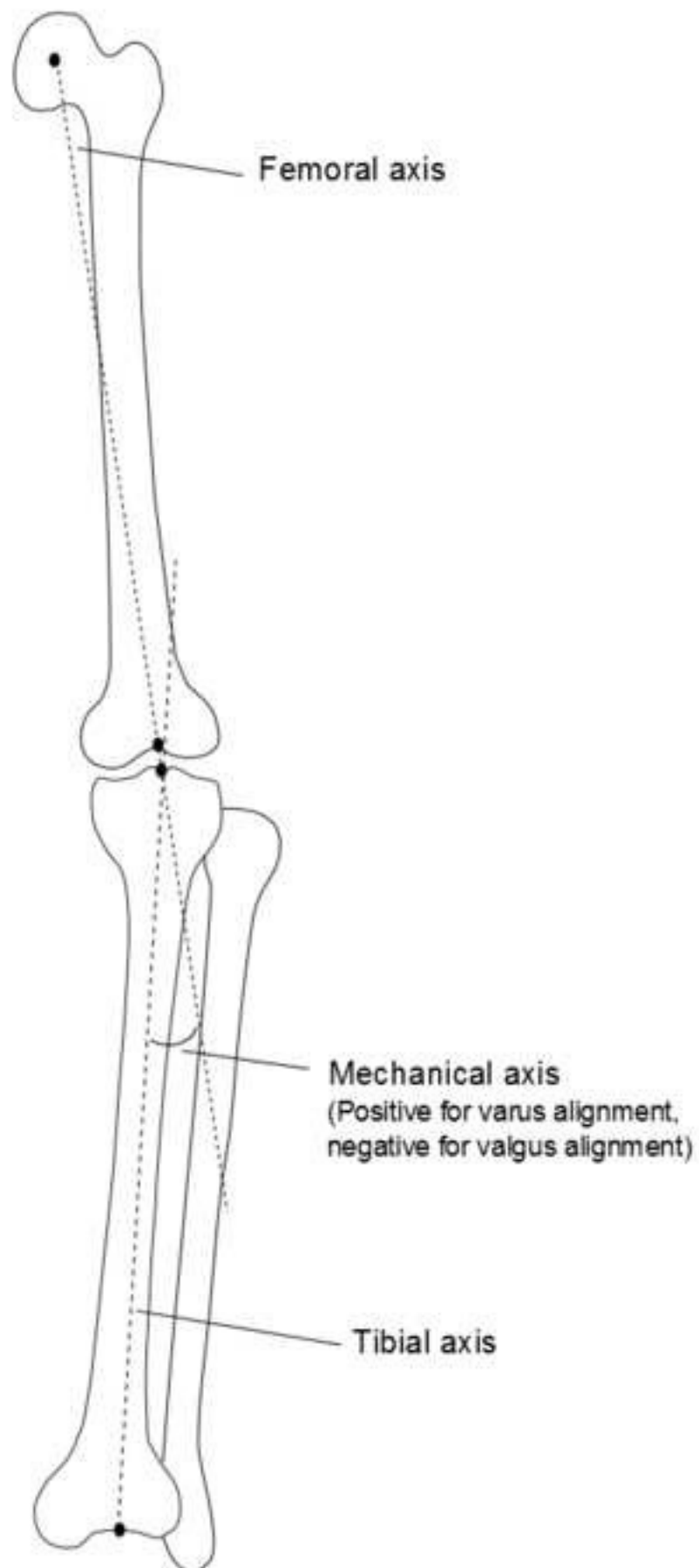


Figure 1



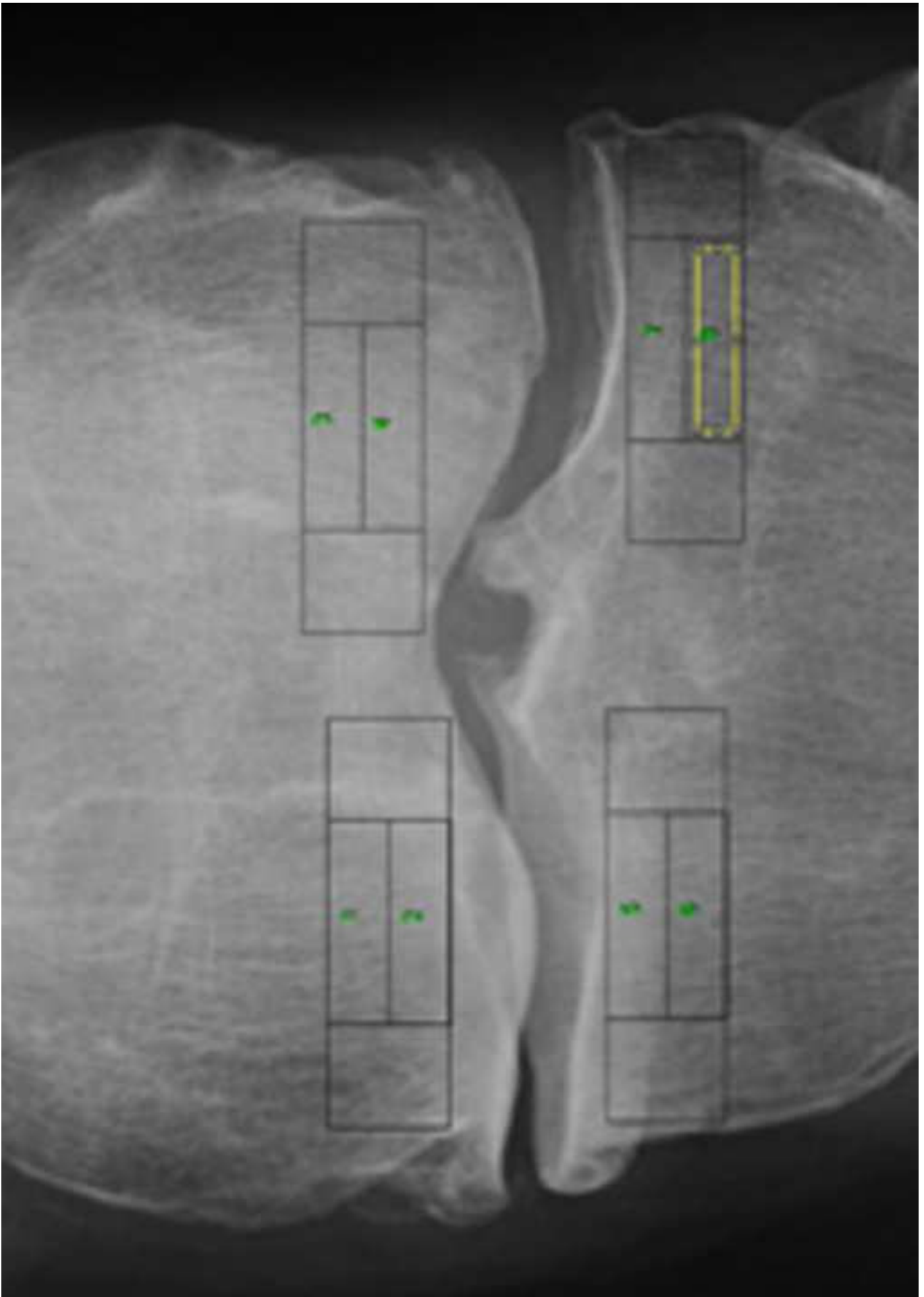


Figure 3

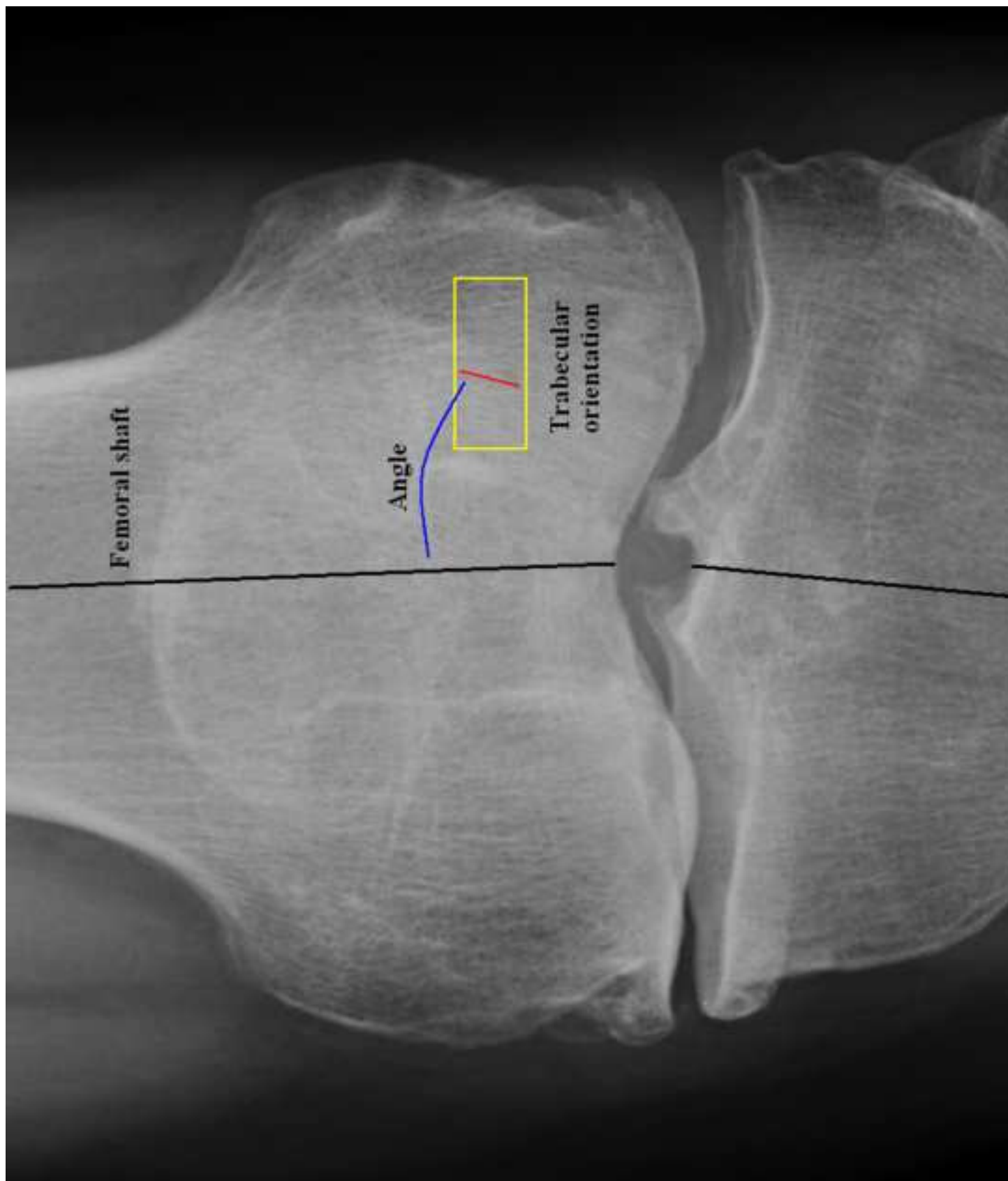
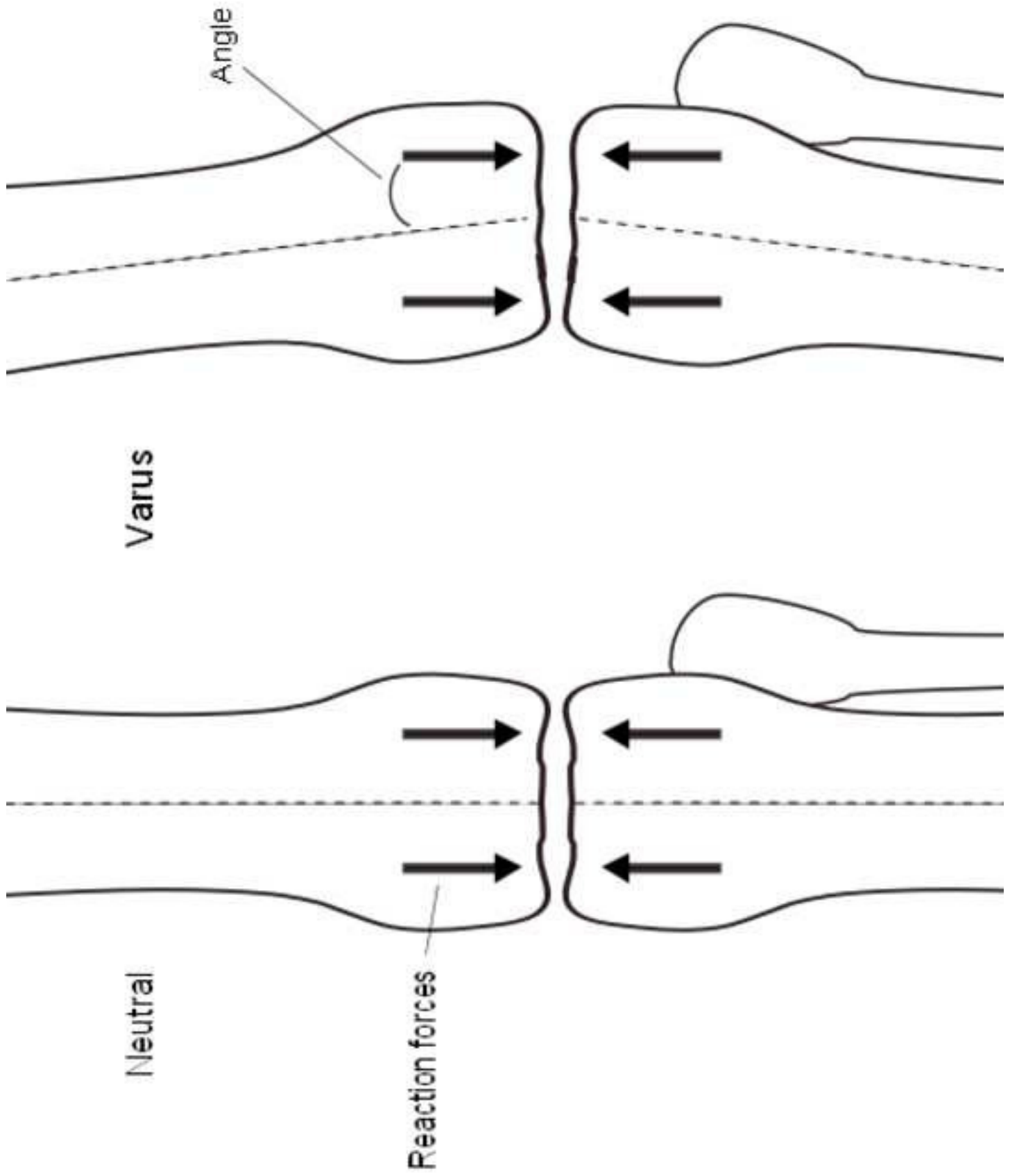


Figure 4



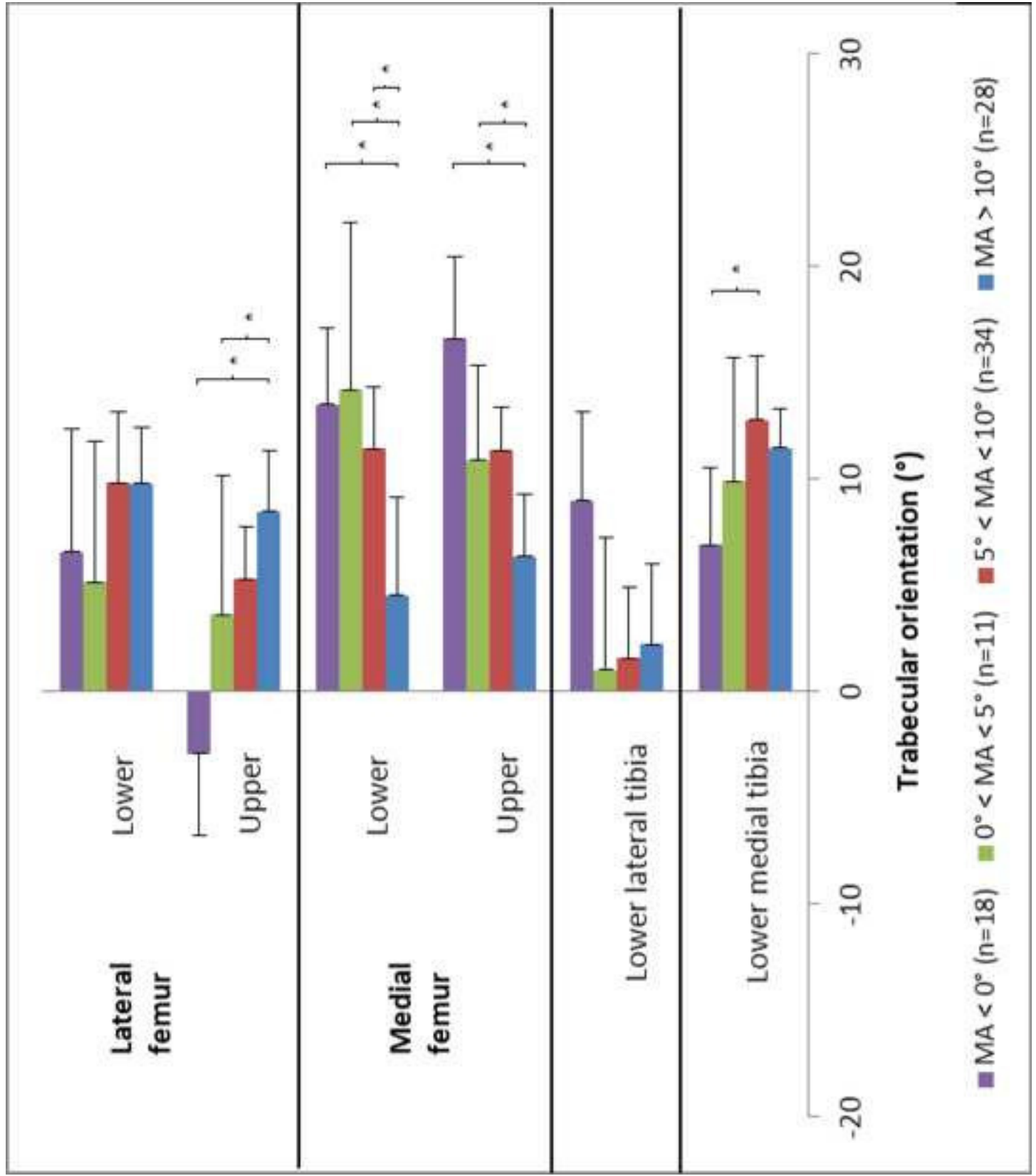


Figure 6